pacemaker output. Nat Neurosci 9: 1041-1049.

28. Aguilar-Roblero R, Mercado C, Alamilla J, Laville A, Díaz-Muñoz M (2007) Ryanodine receptor Ca^{2+}-release channels are an output pathway for the circadian clock in the rat suprachiasmatic nuclei. Eur J Neurosci 26: 575-582.

29. Wang Z, Tymianski M, Jones OT, Nedergaard M (1997) Impact of cytoplasmic calcium buffering on the spatial and temporal characteristics of intercellular calcium signals in astrocytes. J Neurosci 17: 7359-7371.

30. Grant SK, Bansal A, Mitra A, Feighner SD, Dai G, et al. (2001) Delay of intracellular calcium transients using a calcium chelator: application to high-throughput screening of the capsaicin receptor ion channel and G-protein-coupled receptors. Anal. Biochem 294: 27-35.

31. Miyawaki A, Griesbeck O, Hiem R, Tsien RY (1999) Dynamic and quantitative Ca^{2+} measurements using improved cameleons. Proc Natl Acad Sci USA 96: 2135-2140.

32. Silver R, Romero MT, Besmer HR, Leak R, Nunez JM, et al. (1996) calbindin-D28k cells in the hamster SCN express light-induced Fos. Neuroreport 7: 1224-1228.

33. LeSauter J, Silver R (1999) Localization of a suprachiasmatic nucleus subregion regulating locomotor rhythmicity. J Neurosci 19: 5574-5585.

34. Silver R, Sookhoo AI, LeSauter J, Stevens P, Jansen HT, et al. (1999) Multiple regulatory elements result in regional specificity in circadian rhythms of neuropeptide expression in mouse SCN. Neuroreport 10: 3165-3174.

35. Mahoney MM, Nunez AA, Smale L (2000) Calbindin and Fos within the suprachiasmatic nucleus and the adjacent hypothalamus of Arvicanthis Niloticus and Rattus Norvegicus. Neuroscience 99: 565-575.

36. Ikeda M, Allen CN (2003) Developmental changes in calbindin-D28k and calretinin expression in the mouse suprachiasmatic nucleus. Eur J Neurosci 17: 1111-1118.

37. Hamada T, LeSauter J, Lokshin M, Romero M-T, Yan L, et al. (2003) Calbindin influences response to photic input in suprachiasmatic nucleus. J Neurosci 23: 8820-8826.

38. Neher E, Augustine GJ (1992) Calcium gradients and buffers on bovine chromaffin cells. J Physiol (Lond) 450: 273-301.

39. Regehr WD, Tank DW (1992) Dendritic calcium dynamics. Curr Opin Neurobiol 4: 373-382.

40. Neher E (1995) The use of fura-2 for estimating Ca^{2+} buffers and Ca^{2+} fluxes. Neuropharmacology 34: 1423-1442.

41. Pennartz CM, Geurtsen AMS, De Jeu MTG., Sluiter AA, Hermes MHLJ (1998) Electrophysiological and morphological heterogeneity of neurons in slices of rat suprachiasmatic nucleus. J Physiol (London) 506: 775-793.

42. Laemle LK, Hori N, Strominger NL, Tan Y, Carpenter DO (2002) Physiological and anatomical properties of the suprachiasmatic nucleus of an anophthalmic mouse. Brain Res 953: 73-81.

Figure Legends

Figure 1. Spontaneous Ca^{2+} spikes in rat acute SCN slices: Phase contrast image (A) and fluo-4 AM (20 μM) stained fluorescent image (B) of a hypothalamic brain slice containing rat SCN (scale bar, 200 μm). (C and D) Time series of spontaneous $[Ca^{2+}]_c$ spiking activities of SCN neurons obtained at ZT 6 and ZT 18 (scale bar, 50 μm). Each colored circular mark in C and D matches with the time series shown in the same color. The bandwidth of each calcium spike varies significantly from one cell to the other, typically ranging from 5–60 seconds (cf. graph in inset). (E) The mean frequency of spontaneous Ca^{2+} spikes in SCN as a function of zeitgeber time. Each dot marks the mean frequency of the Ca^{2+} spikes exhibited by one cell during a period of 800–1000 sec. The data were collected from the $[Ca^{2+}]_c$ active cells in 1–3 different slices each hour, totaling 475 cells.

Figure 2. None or fewer Ca^{2+} spiking activities in cultured SCN cells that express yellow cameleon: (A) Comparison of cell populations that displayed spontaneous Ca^{2+} spikes in different SCN preparations. The fluo-4 AM-loaded rat acute slice (rat AS + fluo-4 AM) contains Ca^{2+} spiking cells in 18% of the total cells (as in Fig. 1). This ratio

was significantly larger than that in rat slice cultures (rat SC) or in mouse slice cultures (mouse SC). $**P < .01$ by one-way ANOVA. The slice cultures that express yellow cameleon with CMV promoter (+pCMV/YC) had slightly larger number of Ca^{2+} spiking cells in comparison with those that express yellow cameleon with NSE promoter (+pNSE/YC), but the difference was not statistically significant. An example fluorescent image of mouse SC + pNSE/YC is shown on the left (scale bar, 50 μm). (B) Long-term traces (sampling rate at 1 frame per 10 min) of the level of $[Ca^{2+}]_c$ in three different SCN neurons in the mouse SC + pNSE/YC represent robust circadian oscillations. The imaging done at the higher sampling rate (1 frame per 3 seconds) was taken at the approximate plateau (C) and trough (D) of the circadian $[Ca^{2+}]_c$ rhythms, with no $[Ca^{2+}]_c$ spiking activities being detected in these SCN neurons.

Figure 3. The effect of fluo-4 AM and BAPTA AM on the $[Ca^{2+}]_c$ level of rat SCN cells expressing cameleon (pCMV/YC): The transmitted-light image (A) and fluorescent-light image (B) of a hypothalamic slice culture showing a pair of SCN (scale bar, 200 μm). This particular slice culture contained approximately 70–90 cameleon-expressing SCN cells. The cameleon-expressing cells were recorded for 450 seconds under the circulation of oxygen-saturated ACSF. Then the same samples were

incubated under the ACSF containing 2.5-μM fluo-4 AM (C) or BAPTA AM (D) for 15 minutes, washed, and recorded again for another 500 seconds. None of the cells expressing cameleon had spontaneous Ca^{2+} spikes before the treatment with fluo-4 AM or BAPTA AM, but approximately 13~15% (17 out of 118 cameleon-expressed cells in a fluo-4 AM-treated sample, 20 out of 155 cells in a BAPTA AM-treated sample) of the cameleon-expressing cells exhibited Ca^{2+} spikes after the treatment with fluo-4 AM or BAPTA AM. (C) and (D) are a typical example of the responding cells.

Figure 4. The loading effect of fluo-4 Ca^{2+} indicator dye on the AP firing activity of a SCN neuron: (A) A typical spontaneous firing pattern and the time trace of mean firing rate of a SCN neuron in an acute rat hypothalamic slice. (B) The time trace of mean firing rate (black) and the level of $[Ca^{2+}]_c$ (green) of a SCN neuron following the fluo-4 AM dye injection (100 μM). The mean firing rate is computed based on a 10-second sliding window. The time "0" denotes the onset of the whole-cell mode. (C) Time series of AP spiking activities during the fluo-4 AM dye loading as marked in B. The red dashed lines guide the resting membrane potential.

Figure 5. Heterogeneous response of SCN cells to the increasing concentration of

fluo-4 AM in rat slice cultures of SCN: The dependency of spontaneous $[Ca^{2+}]_c$ spiking activity on the concentration (0.5–10 μM) of fluo-4 AM was examined. The mean frequency of calcium spikes was gradually increased in about 49% (A-B) of the active populations, had no systematic change in 35% (C-D), and decreased in 16% (E-F). The red crosses mark the peak positions. All error bars represent a standard error. The data were collected from a total of 76 active cells in 3 different slices. A, C, and E are three representative cases corresponding to the three different subpopulations.

Tables

Table 1. The change of the resting membrane potential of SCN neurons induced by fluo-4 dye loading.

fluo-4 concentration	*> 150 μM*	*80~120 μM*	*< 60 μM*
Number of neurons	n=8/8	n=9/18	n=10/10
Initial *Vm (mV)*	-43.7 ± 1.6	-43.4 ± 0.8	-43.2 ± 2.1
Steady state *Vm (mV)*	Unstable	-46.3 ± 1.3*	-41.7 ± 2.0

'Initial' and 'steady state' refer to the first 30 seconds of dye loading and the time just before the emergence of the first Ca^{2+} spike, respectively. The given values represent mean±SEM. * $p < 0.05$, t-test.

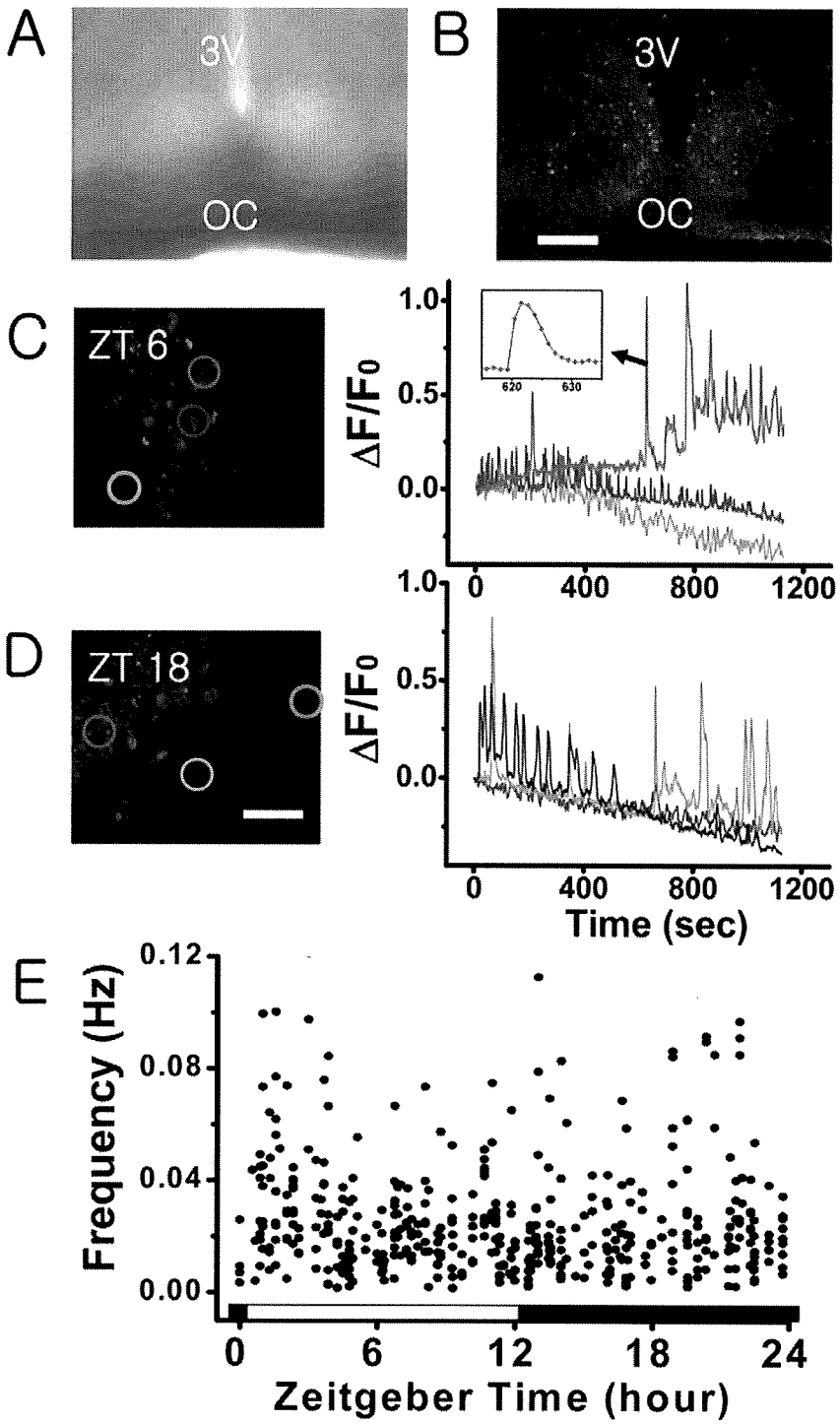
A
3V
OC
B
3V
OC
C
ZT 6
D
ZT 18
ΔF/F0
1.0
0.5
0.0
620
630
0
400
800
1200
Time (sec)
E
Frequency (Hz)
0.12
0.08
0.04
0.00
0
6
12
18
24
Zeitgeber Time (hour)

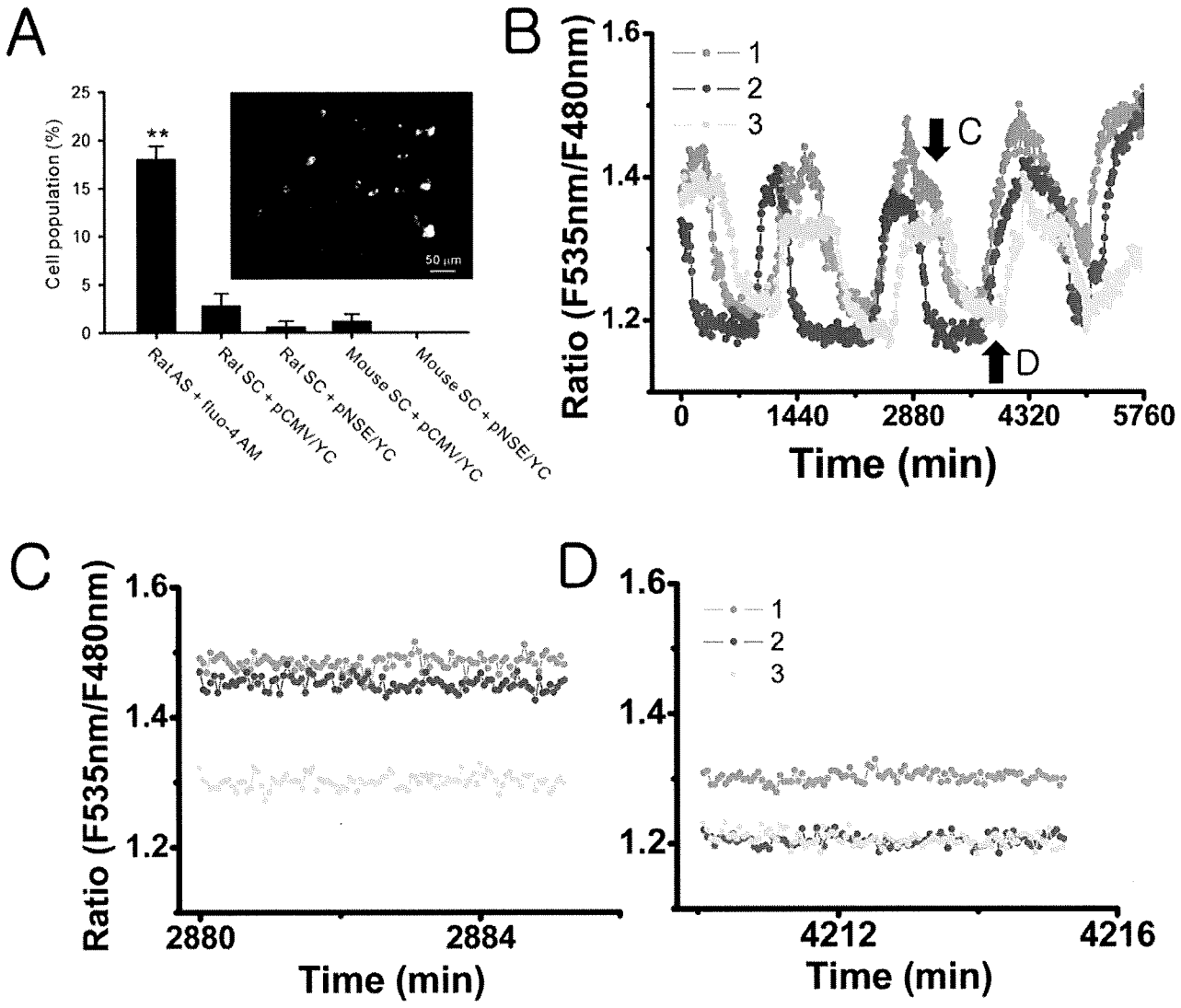
A
Cell population (%)
25
20
15
10
5
0
**
50 μm
Rat AS + fluo-4 AM
Rat SC + pCMV/YC
Rat SC + pNSE/YC
Mouse SC + pCMV/YC
Mouse SC + pNSE/YC
B
Ratio (F535nm/F480nm)
1.6
1.4
1.2
1
2
3
C
D
0
1440
2880
4320
5760
Time (min)
C
Ratio (F535nm/F480nm)
1.6
1.4
1.2
2880
2884
Time (min)
D
1.6
1.4
1.2
1
2
3
4212
4216
Time (min)

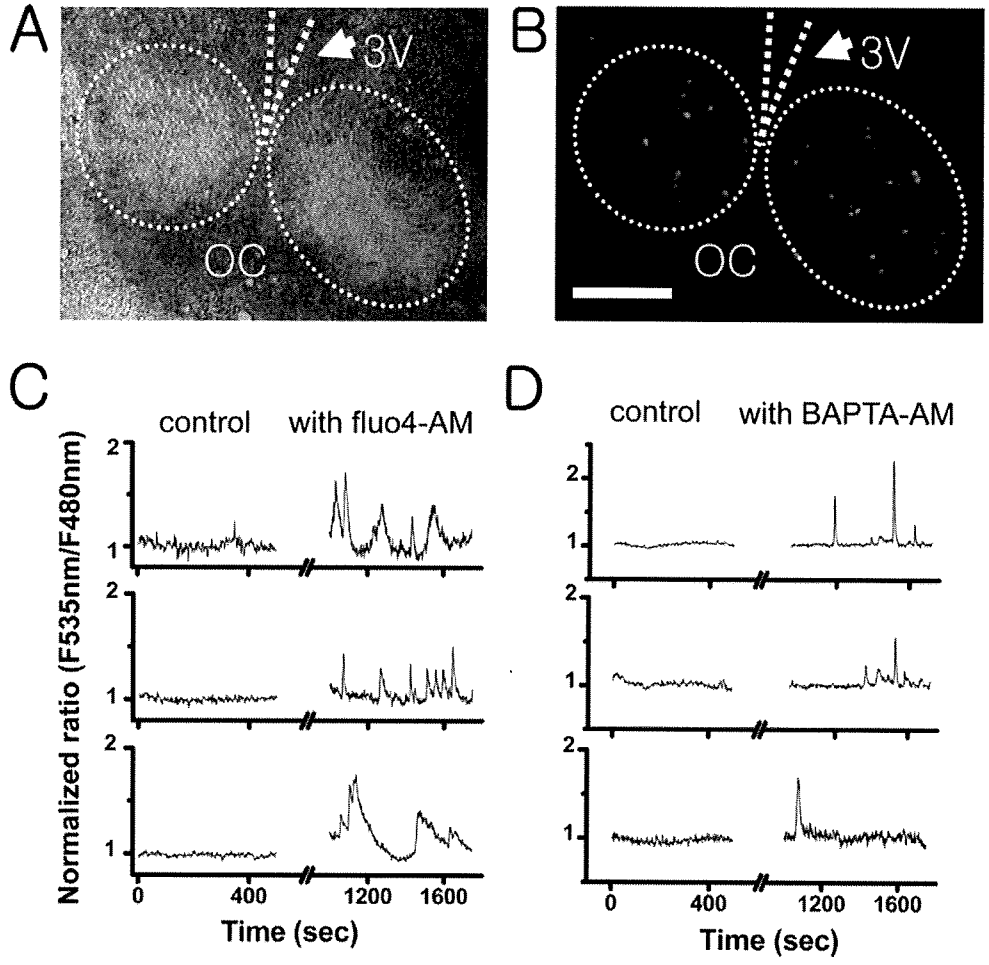
A
3V
OC
B
3V
OC
C
control
with fluo4-AM
Normalized ratio (F535nm/F480nm)
2
1
0
400
1200
1600
Time (sec)
D
control
with BAPTA-AM
2
1
0
400
1200
1600
Time (sec)

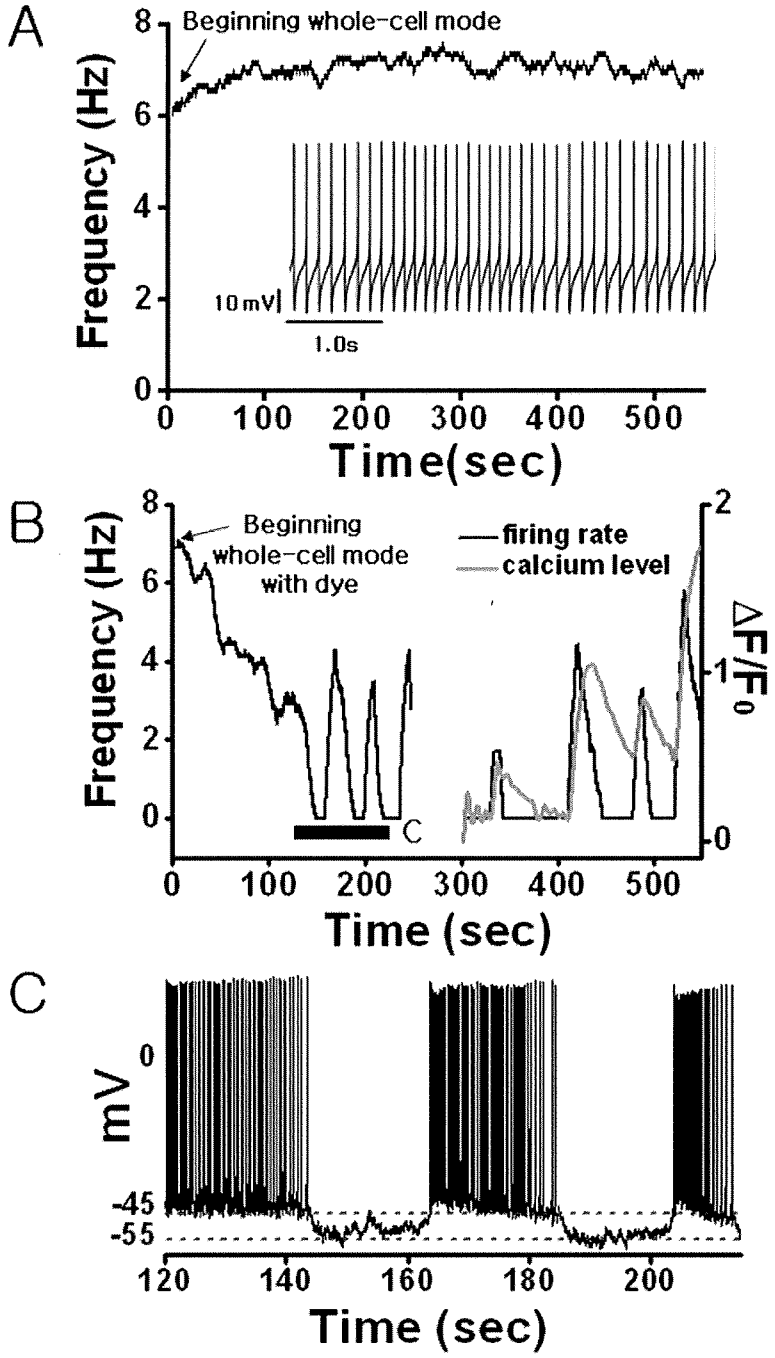
A
Beginning whole-cell mode
Frequency (Hz)
10 mV
1.0s
Time(sec)
B
Beginning
whole-cell mode
with dye
firing rate
calcium level
Frequency (Hz)
ΔF/F0
C
Time (sec)
C
mV
-45
-55
Time (sec)

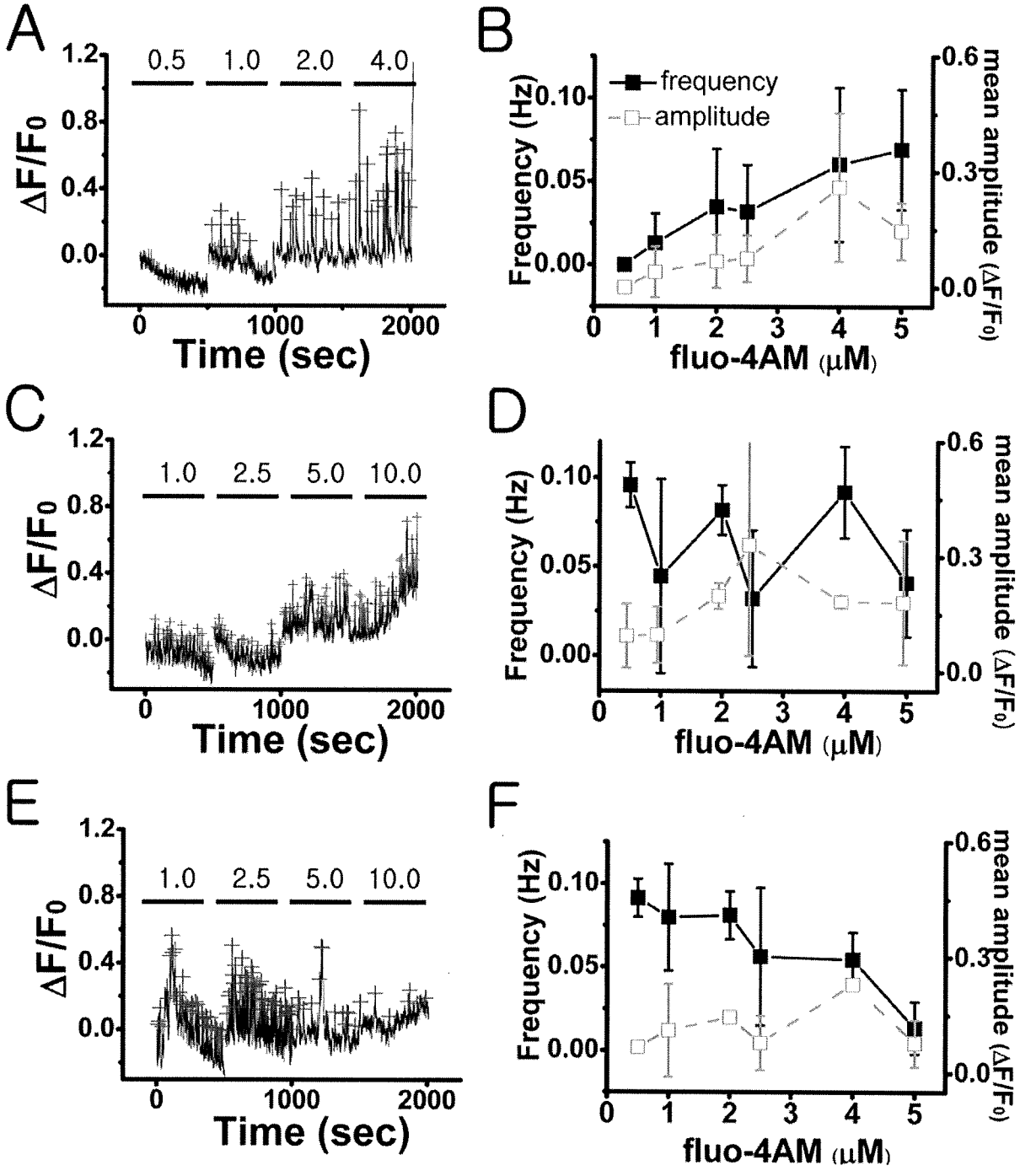
A
0.5
1.0
2.0
4.0
ΔF/F0
Time (sec)
B
frequency
amplitude
Frequency (Hz)
mean amplitude (ΔF/F0)
fluo-4AM (μM)
C
1.0
2.5
5.0
10.0
ΔF/F0
Time (sec)
D
Frequency (Hz)
mean amplitude (ΔF/F0)
fluo-4AM (μM)
E
1.0
2.5
5.0
10.0
ΔF/F0
Time (sec)
F
Frequency (Hz)
mean amplitude (ΔF/F0)
fluo-4AM (μM)

Supporting Information

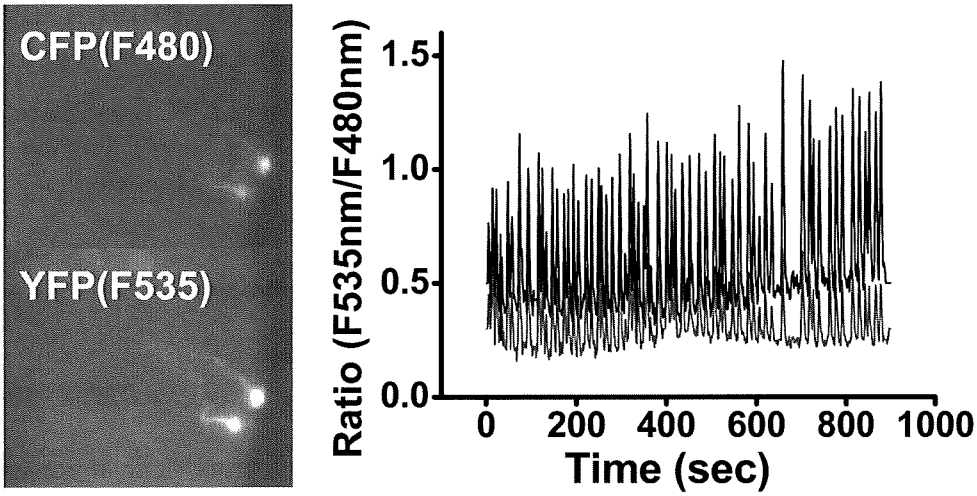

Figure S1 Spontaneous Ca^{2+} spiking activities in cultured rat hypothalamic neurons that express yellow cameleon (pNSE/YC): Time series (sampling rate at 1 frame per 1.5 seconds) of the level of $[Ca^{2+}]_c$ in two different hypothalamic neurons exhibit robust synchronized Ca^{2+} spiking activities .

Optical recording of neuronal activity with a genetically-encoded Ca^{2+} indicator in anesthetized and freely moving mice

Henry Lütcke[1,10], Masanori Murayama[2,3,10], Thomas Hahn[4,5], David J. Margolis[1], Simone Astori[4,6], Stephan Meyer zum Alten Borgloh[4], Werner Göbel[1], Ying Yang[4], Wannan Tang[4], Sebastian Kügler[7], Rolf Sprengel[4], Takeharu Nagai[8,9], Atsushi Miyawaki[8], Matthew E. Larkum[2], Fritjof Helmchen[1*], Mazahir T. Hasan[4*]

[1]Department of Neurophysiology, Brain Research Institute, University of Zurich, Zurich, Switzerland
[2]Department of Physiology, University of Bern, Bern, Switzerland
[3]Behavioral Neurophysiology Laboratory, Brain Science Institute, RIKEN, Wako, Saitama, Japan
[4]Department of Molecular Neurobiology, Max Planck Institute for Medical Research, Heidelberg, Germany
[5]Department of Psychiatry, Central Institute for Mental Health, Mannheim, Germany
[6]Department of Cell Biology and Morphology, University of Lausanne, Lausanne, Switzerland
[7]University of Göttingen Medical School, Göttingen, Germany
[8]Laboratory for Cell Function Dynamics, Brain Science Institute, RIKEN, Wako, Saitama, Japan
[9]Research Institute for Electronic Science, Hokkaido University, Hokkaido, Japan

[10]These authors contributed equally to this work

[*]Corresponding authors:

Mazahir T. Hasan
Department of Molecular Neurobiology
Max Planck Institute for Medical Research
Jahnstrasse 29
D-69120 Heidelberg
Germany
Phone +49-6221-486617
Fax +49-6221-486110
mazahir.hasan@mpimf-heidelberg.mpg.de

Fritjof Helmchen
Department of Neurophysiology
Brain Research Institute
University of Zurich
Winterthurerstrasse 190
CH-8057 Zurich
Phone +41-44-6353340
Fax +41-44-6353303
helmchen@hifo.uzh.ch

Running Title: "Imaging neuronal activity with YC3.60"

Keywords: calcium, yellow cameleon, neocortex, two-photon microscopy, adeno-associated virus, barrel cortex

Abstract

Fluorescent calcium (Ca^{2+}) indicator proteins (FCIPs) are promising tools for functional imaging of cellular activity in living animals. However, they have still not reached their full potential for in vivo imaging of neuronal activity due to limitations in expression levels, dynamic range, and sensitivity for reporting action potentials. Here, we report that viral expression of the ratiometric Ca^{2+} sensor yellow cameleon 3.60 (YC3.60) in pyramidal neurons of mouse barrel cortex enables in vivo measurement of neuronal activity with high dynamic range and sensitivity across multiple spatial scales. By combining juxtacellular recordings and two-photon imaging in vitro and in vivo, we demonstrate that YC3.60 can resolve single action potential (AP)-evoked Ca^{2+} transients and reliably reports bursts of APs with negligible saturation. Spontaneous and whisker-evoked Ca^{2+} transients were detected in individual apical dendrites and somata as well as in local neuronal populations. Moreover, bulk measurements using wide-field imaging or fiber-optics revealed sensory-evoked YC3.60 signals in large areas of the barrel field. Fiber-optic recordings in particular enabled measurements in awake, freely moving mice and revealed complex Ca^{2+} dynamics, possibly reflecting different behavior-related brain states. Viral expression of YC3.60 - in combination with various optical techniques - thus opens a multitude of opportunities for functional studies of the neural basis of animal behavior, from dendrites to the levels of local and large-scale neuronal populations.

1. Introduction

Neuronal circuits are organized at diverse spatial scales, from sub-cellular compartments such as dendrites to local neuronal populations to whole brain areas. For understanding how information is encoded in neuronal circuits, it is essential to record activity from a large number of neurons in living and, preferably, in freely moving animals. Advanced in vivo fluorescence staining and imaging techniques, in particular using fluorescent Ca^{2+} indicators, permit functional studies of neuronal activity in the living brain across all spatial scales (Grewe and Helmchen, 2009; Helmchen and Denk, 2005; Kerr and Denk, 2008; Wilt et al., 2009). Because action potentials induce Ca^{2+} transients in soma and dendrites via opening of voltage-gated Ca^{2+} channels (Helmchen et al., 1996; Markram and Sakmann, 1994), neuronal spiking activity can be inferred from the fluorescence measurements. Introduction of synthetic Ca^{2+} indicators into cells by patch-pipettes have enabled high-resolution Ca^{2+} measurements from single neurons and their dendrites by in vivo two-photon imaging (Helmchen et al., 1999; Svoboda et al., 1997; Waters et al., 2003). Probing of neuronal network activity in vivo became possible by a multi-cell bolus loading technique with membrane-permeant Ca^{2+} indicators (Kerr et al., 2005; Stosiek et al., 2003), enabling for example the study of the functional organization of sensory-evoked neuronal population responses in the rodent barrel cortex (Kerr et al., 2007; Sato et al., 2007). In addition, large-scale measurements of regional activation (without cellular resolution) can be performed by single-photon excitation and wide-field epifluorescence imaging (Berger et al., 2007) or fiber-optic bulk recording (Adelsberger et al., 2005). A great advantage of the latter approach is that it permits measurements in awake and freely moving animals (Murayama and Larkum, 2009a; Murayama et al., 2007; Murayama et al., 2009). In spite of their strengths, synthetic Ca^{2+} indicators have disadvantages and limitations. In particular, they cannot label specific subpopulations of cells and subcellular compartments. Moreover, synthetic dye loading is not stable over

time and potentially damaging to the brain tissue, limiting the duration of imaging to a few hours.

Genetically-encoded fluorescent Ca^{2+} indicator proteins (FCIPs) (Hires et al., 2008; Mank and Griesbeck, 2008; Miyawaki et al., 2005; Palmer and Tsien, 2006) allow for long-term, cell-type specific imaging of neural activity in living animals. Following the introduction of the first Ca^{2+}-sensitive protein indicator 'cameleon' over a decade ago (Miyawaki et al., 1997), great progress has been made in developing improved FCIPs for functional expression in the mammalian brain (Hasan et al., 2004; Heim et al., 2007; Mank et al., 2008; Nagai et al., 2004; Tian et al., 2009; Wallace et al., 2008). First generations of 'yellow cameleons' (YC) showed functional responses in cultured mammalian cells and in invertebrates but their performance in mammalian neurons in an intact tissue was disappointing (Hasan et al., 2004), possibly due to (a) poor fluorescence-resonance-energy-transfer (FRET) efficiency in response to Ca^{2+} increases and (b) potential interaction of Ca^{2+} sensing domains in YCs with cellular targets. Subsequently, the use of a circular permuted Venus 173 variant (cpVenus 173) as a yellow fluorescent protein (YFP) FRET partner of cyano fluorescent protein (CFP) produced a YC sensor, YC3.60, that showed efficient FRET responses with a large dynamic range in cuvette and also in cultured HeLa cells (Nagai et al., 2004). Moreover, to reduce interaction of Ca^{2+} sensing modules with cellular targets, mutant CaM/M13 pairs and the skeletal muscle specific Ca^{2+} sensing protein troponin were used to engineer novel YCs, D3cpv (Palmer et al., 2006) and TN-XXL (Mank et al., 2008), respectively. In D3cpv, cpVenus 173 was used with CFP while in TN-XXL a circular permuted Citrine 174 was used with CFP. All three FCIPs, YC3.60 (Kuchibhotla et al., 2008; Nagai et al., 2004), D3cpv (Palmer et al., 2006; Wallace et al., 2008) and TN-XXL (Mank et al., 2008) have been shown to be functional in vivo. Unlike for D3cpv and TN-XXL, however, functional characterization of YC3.60 has remained incomplete. Since these three FCIPs have the circular permuted YFP variants, cpVenus173 (YC3.60 and D3cpv) and cpCitrine 174 (TN-XXL), as a key feature in common, it appeared promising to further examine the suitability of YC3.60 for in vivo imaging of neural activity and deploy recombinant adeno-associated viruses (rAAVs) as a method of gene delivery that has been successfully applied in previous studies (Tian et al., 2009; Wallace et al., 2008).

Here, we report that viral expression of YC3.60 in the mouse barrel cortex allows in vivo measurements of spontaneous and whisker-evoked neuronal activity with high sensitivity and dynamic range. In combination with two-photon microscopy, YC3.60 permits Ca^{2+} measurements from individual apical dendrites of cortical neurons as well as from small populations of neurons. Moreover, we demonstrate that YC3.60 Ca^{2+} signals in barrel cortex can be read out in a bulk fashion, in particular through an optical fiber, which enables optical recording of neocortical activity during behavior in freely moving mice. Based on the excellent in vivo performance of virally-expressed YC3.60, we propose it as a sensitive and versatile tool for optical studies of brain function.

2. Materials and Methods

All experiments were performed in accordance with the animal welfare guidelines of the

Max Planck Society and the guidelines of the Federal Veterinary Office of Switzerland, respectively. All experimental procedures were approved by the local authorities (Regierungspräsidium Karlsruhe and Cantonal Veterinary Offices in Zurich and Bern, respectively).

2.1. AAV-mediated gene transfer into mouse neocortex

Recombinant adeno-associated virus (rAAV) equipped with YC3.60 under control of a human synapsin promoter was co-transfected with pDp1, pDp2 (ratio: 3:1) helper plasmids in HEK293 cells (Hasan et al., 2004; Tian et al., 2009; Wallace et al., 2008). Seventy-two hours after transfection, HEK293 cells were collected and packaged viruses were released by repeated freeze-and-thaw on dry-ice-ethanol bath. Viruses were purified first on the iodixanol gradient and later by pre-casted 1 ml Heparin columns (Amersham) using FPLC (Kugler et al., 2007). Infectious virus titers were determined in primary neuron cultures and was 3 x 10^8 transducing units per microliter. Before virus injection, 6-8 weeks old BL/C57 mice were anesthetized with ketamine plus xylazine by intraperitoneal injection (ketamine, 80 mg per kilogram body weight; xylazine, 10–16 mg/kg). Viruses (200-300 nl) were delivered through thin glass pipettes (tip size 8–12 μm) at a depth of about 250 μm to the whisker-related somatosensory cortex (L2/3) by stereotaxic injection (Hasan et al., 2004; Tian et al., 2009; Wallace et al., 2008). To facilitate intraparenchymal administration we included 20% hypertonic D-mannitol in the solution (Mastakov et al., 2001). Infected animals were kept for at least 21 days before imaging or analysis of brain tissues.

2.2. Tissue fixation and immunohistochemistry

Mouse brains were fixed for a few hours in 4% paraformaldehyde and YFP fluorescence was visualized as a bright spot at the virus-injection site using a stereomicroscope (SV11; Zeiss). Brains were coronally sliced to a thickness of 75-100 μm using a vibratome (VT 1000S; Leica Instruments). Slices were counterstained for neuron-specific marker, NeuN, using a mouse anti-neuronal nuclei (NeuN) monoclonal antibody (1:1,000 dilution) (Millipore) and a Cy3-conjugated goat anti-mouse IgG (1:200 dilution; Jackson Immuno Research laboratories). Green (GFP) and red (Cy3) fluorescence were visualized with the Zeiss LSM 5 Pascal laser scanning confocal imaging system equipped with GFP filters.

2.3. Ca^{2+} imaging and electrophysiology in slice cultures

Organotypic hippocampal slices were prepared as previously described (Stoppini et al., 1991) and superfused during recording at room temperature with artificial CSF (ACSF; Biometra) containing (in mM): 125 NaCl, 25 $NaHCO_3$, 2.5 KCl, 1.25 NaH_2PO_4, 1 $MgCl_2$, 2 $CaCl_2$, 25 Glucose, saturated with 95% O_2/5% CO_2. Loose patch-clamp recordings were performed from CA3 pyramidal cells with ACSF-filled pipettes (50-100 MΩ). Cell spiking was elicited by monopolar electrical stimulation delivered at a rate of <0.1 Hz with an ACSF-filled glass pipette placed in the region of the apical dendrites (stratum lucidum or stratum radiatum). Multiple spikes were generated by varying the number of electrical stimuli delivered at 100 Hz. Electrophysiological signals were acquired with a software-controlled patch-clamp amplifier (EPC-9, Pulse 8.11; Heka

Elektronik). For the in vitro characterization of YC3.60 we used hippocampal neurons because hippocampal slice cultures are routinely available in the lab. Neocortical and hippocampal neurons are known to exhibit very similar AP-evoked Ca^{2+} signaling (Helmchen et al., 1996). Two-photon imaging of slice cultures was performed with a mode-locked femtosecond Ti-sapphire laser (Chameleon XR; Coherent) set at an excitation wavelength of 840 nm. Fluorescence signals were acquired with an upright laser scanning microscope (Zeiss LSM 510 NLO) equipped with a 63x water immersion objective (NA 1.0). Frame-scan acquisition was performed from somatic regions of interest (ROIs) at a rate of 24.1 Hz. Frames typically were 30 x 27 pixels (pixel size 140 nm x 140 nm). While ROI width could vary the number of lines was kept constant to ensure the same sampling rate for all recordings.

2.4. In vivo Ca^{2+} imaging and electrophysiology

Animals were surgically prepared for in vivo imaging as described previously (Nimmerjahn et al., 2004; Wallace et al., 2008; Waters et al., 2003). Briefly, mice were anaesthetized with urethane (~1.5 g/kg) and a stainless steel plate was attached to the exposed skull. For experiments combining electrophysiology and imaging the dura was carefully removed. The exposed tissue was superfused with normal rat Ringer solution (in mM: 135 NaCl, 5.4 KCl, 5 HEPES, 1.8 $CaCl_2$, pH 7.2 with NaOH). To dampen heartbeat and breathing-induced motion, we filled the cranial window with agarose (type III-A, Sigma; 1% in NRR) and covered it with an immobilized glass coverslip. Body temperature was maintained at 37°C with the help of a heating blanket. For imaging, we used a custom-built two-photon microscope with ~100-fs laser pulses at 870 nm wavelength provided by a Ti:sapphire laser (Spectra-Physics) and a 40x water-immersion objective (NA 0.8; Olympus). CFP and YFP fluorescence were collected with blue (450 – 475 nm) and green (535 – 550 nm) emission filters (AHF AG). Frame scans were acquired at 7.81 Hz with 128 × 128 pixel resolution. Juxtacellular recordings were obtained from YC3.60-expressing L2/3 neurons with glass pipettes (5–7 MΩ) containing NRR solution and 0.025 mM Alexa-594 for pipette visualization. Neurons were visually targeted using the two-photon microscope. Action potentials were recorded in current-clamp using an Axoclamp 2-B amplifier (Axon Instruments, Molecular Devices) and digitized using software custom-written in LabView (National Instruments).

A commercial camera system (Optical Imaging) and custom made optics were used for wide-field recordings of single-photon excited YFP-fluorescence (excitation filter 440 nm, dichroic mirror 460 nm, emission filter 535 nm). Movies were acquired at 10 Hz from a 4.2 x 4.2 mm field of view and the mean YFP-fluorescence signals from the entire FOV (expressed as relative fluorescence changes $\Delta F/F_{YFP}$) were analyzed during spontaneous activity and upon air-puff whisker stimulation. Control measurements using an emission filter for detecting CFP-fluorescence revealed signal decreases as expected (data not shown). Simultaneous local field potential (LFP) recordings were performed with a 16-site single shank probe (Neuronexustech) on a multichannel recording system (Cheetah, Neuralynx). The probe was inserted under visual control in the middle of the fluorescent spot and LFP signals from L2/3 were recorded.

2.5. Fiber-optic Ca^{2+} recordings

Fiber-optic recordings were performed as described previously (Murayama and Larkum, 2009b; Murayama et al., 2007). Briefly, 8 mice (~ 10 weeks old) were used in these experiments and were deeply anesthetized by isoflurane (1.5-3%, Baxter). Following surgery, an analgesic was administered (buprenorphine, twice per day; Essex Chemie) and local anesthetic (lidocaine; Sigma-Aldrich) applied to the scalp. On the day of the experiment, the head was fixed in a stereotaxic instrument (Narishige) and body temperature maintained at 36°C to 37°C. A craniotomy was performed above the virus injected area (somatosensory barrel cortex, 1 mm diameter.). In one experiment, the skull was thinned above the injected area. The dura mater remained intact. After anesthesia experiments, animals recovered for 1-2 h and were then transferred to the arena for behavioral observation and freely moving fluorescence imaging. Fixation of the fiber-optic mount to the animal's head was performed as described previously (Murayama and Larkum, 2009b). A blue LED (IBF+LS30ROB-3W-Slim-RX or IBF+LS30W-3W-Slim-RX, Imac Co.) was used as a light source. An excitation filter (FF01-438/24-25, Semrock or D480/30x, Chroma Technology), a dichroic mirror (FF520-Di01-25x36, Semrock), and an emission filter (FF01-542/27-25, Semrock) were used for epifluorescence Ca^{2+} recordings. A 10x objective (Edmund Optics) was used for illuminating and imaging an optical fiber (NT57-069, NA, 0.22, core diameter of 440 μm; total diameter of 470 μm, Edmund Optics). A CCD camera (MicroMax, Roper Scientific) was used for collecting fluorescence. Sensory responses were evoked by a brief air puff (50 ms-duration) delivered to the contralateral whiskers. Fluorescence changes were sampled at 100 Hz. Data was acquired on a PC using WinView software (Roper Scientific). ROIs were chosen offline for measuring fluorescence changes (see below). Animal behavior was observed by using a CCD camera (Logitech, Japan). The video recording was acquired and stored to disk using QuickCam software (Logitech). Cadmium chloride was from Fluka.

2.6. Data analysis

For all experiments in slices cultures as well as for in vivo two-photon imaging, Ca^{2+} signals were expressed as relative YFP/CFP ratio changes $\Delta R/R$ after background subtraction and further analyzed using Igor (Wavemetrics Inc.) and Matlab (Mathworks). Peak amplitudes of Ca^{2+} transients were determined as the mean of 3 sampling points around the peak location. Decay time constants were obtained from single-exponential fits. To quantify AP detection, we calculated the signal to noise ratio (SNR) of AP-evoked transients as the ratio of peak amplitude to s.d. of the unfiltered trace 750 ms prior to the first AP. Similarly, the SNR of baseline traces was computed as the ratio of peak to s.d. of the trace. The distribution of baseline SNR values was estimated by fitting a Gaussian and the detection threshold for AP-evoked transients was determined as the SNR value above which less than 5% of baseline traces would be classified as false positives (see Figure 4E). For fiber-optic recordings, fluorescence signals were quantified by measuring the mean pixel value of a manually selected ROI for each frame of the image stack using Igor Pro (Wavemetrics) software. Ca^{2+} changes were expressed as $\Delta F/F = F_t / F_0$, where F_t was the average fluorescence intensity within the ROI at time t during the imaging experiment and F_0 was the mean value of fluorescence intensity before stimulation.